(Hydroxyalkyl)cob(III)alamins as Competitive Inhibitors in Coenzyme B_{12}-Dependent Enzymic Reactions: ^{1}H-NMR Structure Analysis and Kinetic Studies with Glycerol Dehydratase and Diol Dehydratase

by **László Poppe**[a][b], **William E. Hull**[c], **Rainer Nitsche**[a], **Torsten Graf**[a], **Erhard Stupperich**[d], and **János Rétey**[a]*

[a]) Department of Biochemistry, Institute of Organic Chemistry, University of Karlsruhe, Richard-Willstätter-Allee 2, D-76128 Karlsruhe; fax: + 49-721-6084823; e-mail: biochem@ochhades.chemie.uni-karlsruhe.de

[b]) Chemical Research Center, Institute for Chemistry, Hungarian Academy of Sciences, Pusztaszeri út 59–67, H-1025 Budapest

[c]) Central Spectroscopy Department, German Cancer Research Center, Im Neuenheimer Feld 280, D-69120 Heidelberg

[d]) Applied Microbiology, University of Ulm, Albert-Einstein-Allee 11, D-89070 Ulm

A series of (hydroxyalkyl)cobalamins, *i.e.*, **1a**–**d**, (HO–$(CH_2)_n$–Cbl, $n = 2-5$), two diastereoisomeric (2,3-dihydroxypropyl)cobalamins, *i.e.*, **2a**,**b** ([(*R*)- and (*S*)-[$(HO)_2$pr]-Cbl) and their diastereoisomeric 'base-off' analogues, the (*Coβ*-2,3-dihydroxypropyl-[1′-*O*-(*p*-tolyl)cobamides]) **3a**,**b** ([(*R*)- and (*S*)-$(HO)_2$pr]-PTC) were prepared and characterized by their 500-MHz ^{1}H-NMR spectra. The inhibitory activities of these compounds and of hydroxocobalamin (HO–Cbl) and (Co*α*-cyano)(Co*β*-hydroxo)[1′-*O*-(*p*-tolyl)cobamide] (HO–PTC) were tested with two coenzyme-B_{12}-dependent enzymes: glycerol dehydratase (GDH) and propane-1,2-diol dehydratase (DDH) (*Table 4*). The hydroxyalkyl and dihydroxypropyl derivatives of cobalamin acted as strong competitive inhibitors of coenzyme B_{12} (5′-deoxy-5′-adenosylcobalamin, Ado–Cbl) for both enzymes, with K_i values falling within the range defined by HO–Cbl (best inhibitor) and CN–Cbl (K_i/K_m ratio of *ca.* 2). The short-chain HO–$(CH_2)_n$–Cbl (**1a**,**b**; $n = 2$ or 3) exhibited K_i equal to the K_m for Ado–Cbl. The [(*R*)- and (*S*)-$(HO)_2$pr]–Cbl (**2a**,**b**) and the long-chain HO–$(CH_2)_n$–Cbl (**1c**,**d**; $n = 4, 5$) were less efficient inhibitors, with [(*S*)-$(HO)_2$pr]–Cbl (**2a**) performing slightly better than the (*R*)-diastereoisomer **2b** for both enzymes. The 'base-off' analogues, Ado–PTC and [(*R*)- and (*S*)-$(HO)_2$pr]–PTC (**3a**,**b**), were moderate inhibitors with K_i/K_m ratios of 4.5–28 for GDH or 7–13 for DDH. [(*S*)-$(HO)_2$pr]–PTC (**3a**) was the best inhibitor in this group. The non-alkylated analogue (HO,CN)–PTC proved to be a very poor inhibitor. These results confirm that the 'base-on' binding mode of coenzyme B_{12} is preferred for GDH and DDH. The increase in K_i for PTC- *vs.* Cbl-type inhibitors may result from the entropic penalty required for folding of the PTC nucleotide chain into a Cbl-like loop conformation. Hydrophilic interactions between the *β*-ligand of the inhibitor and ribosyl- or substrate-binding sites may make an important contribution to the formation or stabilization of the apoenzyme-inhibitor complex, especially for the PTC derivative.

Introduction. – In several enzyme-catalyzed rearrangements, coenzyme B_{12} (Ado–Cbl; Ado = 5′-deoxy-5′-adenosyl) plays an essential role as a cofactor [1–5]. The common initial step in these reactions is the homolysis of the bond between the Co-atom and C(5′) of the adenosyl ligand on the *β*-face of the cofactor, leading to highly reactive radical intermediates which initiate the rearrangement of the substrate. It has been assumed that the energy required for this homolysis originates from a conformational change in the protein induced by binding of the substrate.

Coenzyme-B_{12}-dependent enzymes may bind their cofactor in two different ways. In the 'base-on' mode, the original 5,6-dimethylbenzimidazolyl moiety of the lower

nucleotide loop of Ado–Cbl remains as the α-ligand of the Co-atom in the enzyme-coenzyme complex. In the 'base-off' binding mode, the 5,6-dimethylbenzimidazolyl moiety is displaced from the Co-atom and a histidine residue of the protein coordinates to the Co-atom as α-ligand.

In the homolysis of the Co–C bond, the nature of the α-ligand attached to the Co-center and the mode of binding of Ado–Cbl to the protein may play a crucial role. It was concluded that for homolysis of the Co–C bond on the β-side, the central Co-atom of the corrin ring should be coordinated by a basic N-atom from the α-side [6][7], *i.e.*, a histidine N-atom from the protein for the 'base-off' enzymes or a 5,6-dimethylbenzimidazole N-atom from Ado–Cbl for the 'base-on' enzymes. On the basis of X-ray crystallography [8][9], EPR spectroscopy using ^{15}N-labeled enzymes and/or coenzymes [10–15], and enzyme kinetics with Ado–PTC[1]) as a 'base-off' analogue of coenzyme B_{12} [16][17], the binding mode for several coenzyme-B_{12}-dependent enzymes has been determined. In the coenzyme-B_{12}-binding region of the 'base-off' enzymes, there is a consensus sequence with a conserved histidine [18–23], but such a sequence similarity is lacking in propanediol and glycerol dehydratases [24][25].

In a previous study, we investigated the interaction of glycerol dehydratase (GDH) and propanediol dehydratase (DDH) with a series of [ω-(adenosin-5′-*O*-yl)alkyl]cobalamins (Ado–O$(CH_2)_m$–Cbl; $m = 3–7$) as possible models or mimics of the posthomolysis intermediate state of coenzyme B_{12} [26]. The hypothesis is that, following bond homolysis, the separation between the Co and adenosyl C(5′) atoms increases due to a conformational change in the enzyme, possibly triggered by substrate binding. Therefore, coenzyme-B_{12} analogues with an increased spacing between the Co-atom and the adenosyl moiety may bind to and stabilize the protein in the posthomolysis conformation. The 'optimal' spacing may depend on the size of the substrate and the geometric relationship between its binding site and the corrin binding site. In agreement with our expectations based on the small size of the substrate for GDH and DDH, the short-chain coenzyme-B_{12} analogues ($m = 3–5$), especially the C_5 analogue ($K_i = 5.9$ and 500 nM for GDH and DDH, resp.), were found to be slightly stronger inhibitors than those with longer chains ($m = 6$ and 7; $K_i = 11.7$ and 15.1 nM resp., for GDH, and 630 and 830 nM, resp. for DDH). In our previous study, the dehydratase-inhibition results obtained with hydroxocobalamin (HO–Cbl) and cyanocobalamin (CN–Cbl) showed interesting features [26]. Although both HO–Cbl and CN–Cbl consist of a cobalamin bearing only a β-ligand of minimal size, their inhibition properties differed significantly. While CN–Cbl with the apolar β-CN ligand proved to be a moderate inhibitor, similar to the long-chain ($m = 6$ and 7) Ado–O$(CH_2)_m$–Cbl posthomolysis-state analogues, HO–Cbl bearing the polar, hydrophilic β-OH ligand was found to be the strongest inhibitor tested for both dehydratases. The ratio of K_i values for HO–Cbl *vs.* CN–Cbl was 0.40 for GDH and 0.48 for DDH, which translates into a binding free energy difference $\Delta\Delta G$ of *ca.* 2.4 kJ/mol in both cases (assuming $\Delta G_{bound} = +RT \ln K_i$).

We rationalized the difference in K_i for HO–Cbl *vs.* CN–Cbl by proposing that HO–Cbl with its hydrophilic β-OH ligand may interact *via* a protein-associated H_2O

---

[1]) The abbreviation PCC (for (*p*-cresolyl)cobamide) was used previously [10][16] to represent the same moiety abbreviated in this work as PTC for [1′-*O*-(*p*-tolyl)cobamide].

molecule with the substrate binding site in addition to the corrin binding site in each dehydratase. The estimated −2.4 kJ/mol difference in ΔG for the binding of HO−Cbl *vs.* CN−Cbl is consistent with the formation of one additional H-bond in the complex. Another possibility is that solvent H_2O tightly associated with the OH ligand of HO−Cbl is displaced upon binding of the inhibitor to the protein, leading to a favorable positive entropy change not available for CN−Cbl.

For the dehydratases, the binding of small, hydrophilic substrates apparently provides an important contribution to the energetics of the catalytic process. Only after addition of substrate to the enzyme-coenzyme-B_{12} complex, EPR signals can be detected (Co−C bond homolysis); these signals also indicate that a conformational change in the ternary complex results in increased separation between the free radical centers [13][14]. The primary OH moiety of propane-1,2-diol or glycerol is not involved in the enzymic rearrangement process; therefore, we assume that it is important for the binding of the substrate of the coenzyme-enzyme binary complex *via* hydrophilic interactions.

Based on these considerations, we decided to investigate several coenzyme-B_{12} analogues with small hydroxyalkyl groups as hydrophilic β-ligands. Our hypothesis was that such analogues may interact with the protein at both the corrin and substrate binding sites and serve as models for a substrate-corrin binding mode, which may mimic a posthomolysis substrate-enzyme-coenzyme complex. Another possibility is that the hydroxyalkyl group may interact with a putative ribose (adenosyl) binding site, which may be important in binding of the natural coenzyme.

In this study, we report the synthesis, the ^{1}H-NMR data, and the enzyme-kinetic behavior of a series of (hydroxyalkyl)cobalamins, *i.e.* **1a**–**d** (HO−$(CH_2)_n$−Cbl, $n = 2$–5), two diastereoisomeric (2,3-dihydroxypropyl)cobalamins, *i.e.*, **2a**,**b** ([(*R*)- and (*S*)−$(HO)_2$pr]−Cbl) and their diastereoisomeric 'base-off' analogues, the (Coβ-2,3-dihydroxypropyl)[1′-*O*-(*p*-tolyl)cobamides] **3a**,**b** [(*R*)- and (*S*)-$(HO)_2$pr]−PTC[1]) (*Fig.*) in the glycerol dehydratase and diol dehydratase reactions. The preparation of [(*R*)- and (*S*)−$(HO)_2$pr]−Cbl (**2a**,**b**) and partial ^{1}H-NMR data have been described earlier by *Dixon et al.* [27], and the X-ray crystal structures [28] are available in the *Cambridge Crystallographic Data Files.*

Results. – The desired (hydroxyalkyl)cobalamins were synthesized from HO−Cbl or its 'base-off' analogue (Coα-cyano)(Coβ-hydroxo)[1′-*O*-(*p*-tolyl)cobamide] (HO−PTC), which differs from vitamin B_{12a} by only the presence of a (*p*-tosyl)oxy moiety instead of the 5,6-dimethylbenzimidazole within the nucleotide loop. The established reductive alkylation method for obtaining alkylated corrinoids from vitamin B_{12a} [29] was used in these reactions as well, and conveniently provided the β-alkylated products (*Fig.*) in good yields.

One- and two-dimensional ^{1}H-NMR spectra were obtained in D_2O at 500 MHz for the two short-chain (hydroxyalkyl)cobalamins **1a**,**b** (HO$(CH_2)_n$−Cbl, $n = 2$ and 3), the two diastereoisomeric 'base-on' dihydroxypropyl derivatives **2a**,**b** and their diastereoisomeric 'base-off' analogues **3a**,**b**. The geminal, vicinal, and long-range coupling information provided by the COSY-β 2D experiment and the spatial information provided by the 2D-NOESY data were sufficient for the unambiguous assignment of all proton signals, with the possible exception of methylene protons at positions C(17[1])

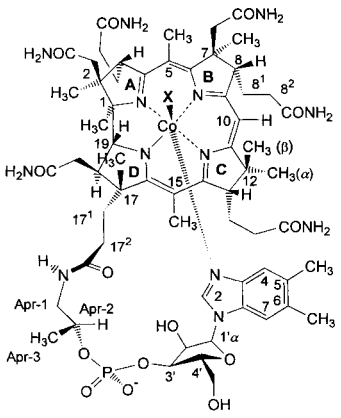

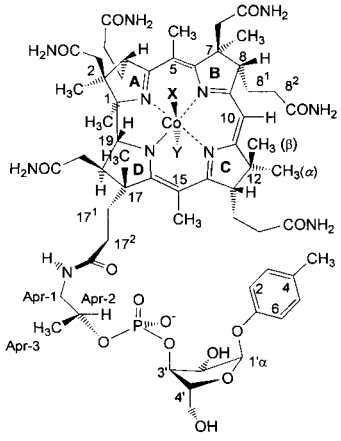

Cbl Derivatives	X
Ado-Cbl	Ado = 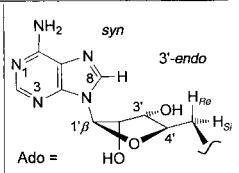
AdoO(CH$_2$)$_m$-Cbl	AdoO(CH$_2$)$_m$ (m = 3-7)
CN-Cbl	CN
HO-Cbl	OH
HO(CH$_2$)$_n$-Cbl (**1a-d**)	HO(CH$_2$)$_n$ (n = 2-5)
[(*S*)-(HO)$_2$pr]-Cbl (**2a**)	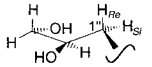
[(*R*)-(HO)$_2$pr]-Cbl (**2b**)	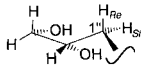

PTC[1] Derivatives	X[a]
Ado-PTC	Ado = 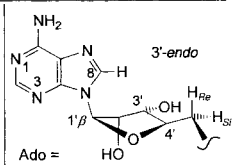
HO-PCC	HO
[(*S*)-(HO)$_2$pr]-PTC (**3a**)	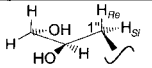
[(*R*)-(HO)$_2$pr]-PTC (**3b**)	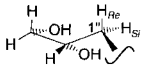

[a]) Ado-PTC: Y = HO; HO–PTC: Y = CN; **3**: Y = HO.

Figure. *Cobalamins* **1a**–**d** *and* **2a**,**b** ((*Coβ*-X)–Cbl) *and 1′*-O (p-*tolyl)cobamides* **3a**,**b** (Co*β*-X)–PTC) *discussed in this work*. Ligands X and Y are on the *β*- and *α*-side of the corrin ring, respectively. The numbering scheme is that used in the NMR tables. For X–Cbl, the configurations and conformations of the corrin substituents, the nucleotide loop, and the adenosyl group are shown as accurately as possible, according to the crystal structure of coenzyme B_{12} (Ado–Cbl) and in agreement with the NMR data. Bonds drawn close to vertical or horizontal directions represent axial or equatorial substituents, respectively. The dimethylbenzimidazole (Dbi) group of the nucleotide loop in Cbl derivatives lies essentially in the perpendicular plane containing the corrin C(5) and C(15) atoms, with the imidazole proton H–C(2) pointing in the direction of the corrin C(15) atom. The ribose conformation of the adenosyl moiety and nucleotide loop of Cbl derivatives is predominantly 'C(3′)-*endo*' (H–C(3′)/H–C(4′) *trans* diaxial), but it is predominantly 'C(2′)-*endo*' (H–C(2′) axial) in the 'base-off' loop region of the PTC derivatives. As X ligand, the adenosyl moiety is oriented with H–C(4′) pointing toward H–C(19) and the *trans* H–C(5′) pointing toward H–C(10). The ribose ring is roughly perpendicular to the corrin ring with the ring O-atom pointing toward C(14)–C(15). The adenine group in '*syn*' orientation is roughly parallel to the corrin and lies over H–C(13) and Me$_\beta$–C(12) with the adenine H–C(8) pointing toward the corrin C(7) atom. The dihydroxypropyl moieties used as X ligands are shown in conformations most closely matching the adenosyl ribose, which has the (*S*)-configuration at C(4′).

The *pro-S* protons at C(1″) and C(3″) in the dihydroxypropyl ligands are drawn with vertical bonds.

and C(17[2]). *Table 1* summarizes the chemical-shift data for four 'base-on' cobalamin compounds in comparison with the data for Ado–Cbl [30][31]. *Table 2* compares the chemical-shift data for the 'base-off' analogues **3a**,**b** with the published data for the 'base-off' form of Ado–Cbl (Ado–′Cbl′) [32] and the 'base-off' analogue Ado–PTC[1]) [16].

A large number of individual geminal and vicinal coupling constants were evaluated in the resolution-enhanced 1D spectra. For the four Cbl analogues **1a**,**b** and **2a**,**b** examined in this study, all resolved couplings for the corrin-ring protons and side chains, as well as the couplings in the aminopropyl and ribose segments of the nucleotide loop, show only minor variations as a function of the β-ligand and agree well with the corresponding values for Ado–Cbl and the 'base-on' Ado–$O(CH_2)_m$–Cbl analogues [29]. As expected, for the two $(HO)_2$pr–PTC 'base-off' derivatives **3a**,**b** those couplings which could be determined deviate in several cases from the couplings observed for 'base-on' Ado–Cbl, especially in the nucleotide loop, but agree well with the corresponding values measured for Ado–PTC [16]. The coupling constants for the hydroxyalkyl β-ligands in the new Cbl and PTC derivatives are unique and are, therefore, summarized in *Table 3*, together with coupling constants for the ribose moieties.

The synthesized compounds were tested as inhibitors in the glycerol dehydratase and diol dehydratase reactions, and the results are summarized in *Table 4*, with the inhibitors arranged roughly in the order of decreasing effectiveness. Assuming that the relative K_i values reflect the relative dissociation constants K_d for the binary inhibitor-enzyme complexes, then a relative free energy for inhibitor binding can be calculated as shown in *Table 4*. All of the (hydroxyalkyl)cobalamins, *i.e.*, those analogues which can be used to model the substrate-enzyme-coenzyme complex that forms with the 'base-on' form of coenzyme B_{12} (Ado–Cbl), proved to be potent competitive inhibitors ($K_i = 13–25$ nM for GDH, 760–1250 nM for DDH) with respect to Ado–Cbl ($K_m =$ 12.6 nM for GDH, 720 nM for DDH). For both enzymes, the short-chain $HO(CH_2)_n$–Cbl analogues **1a**,**b** ($n = 2$ and 3) showed the strongest inhibition with K_i equal within experimental error to the K_m of Ado–Cbl. Introduction of a second OH group to the C_3 alkyl chain reduced the effectiveness of the inhibitors somewhat, *i.e.*, [(*R*)- and (*S*)-$(HO)_2$pr]–Cbl (**2a** and **2b**, resp.) exhibited K_i values of 17.6 and 14.8 nM, respectively, for GDH, and 1250 and 1080 nM, respectively, for DDH. An increase in the chain length as in the monohydroxyalkyl analogues **1c**,**d** ($n = 3$ and 4) also reduced the effectiveness, resulting in K_i values of 17.0 and 25.2 nM, respectively, for GDH, and 1060 and 950 nM, respectively, for DDH.

On the other hand, the dihydroxypropyl derivatives of the 'base-off' corrinato complex PTC were significantly less potent as inhibitors and comparable to Ado–PTC [16], *i.e.*, [(*R*)- and (*S*)-$(HO)_2$pr]–PTC (**3a** and **3b**, resp.) had K_i values of 348 and 57 nM, respectively, for GDH, and 6400 and 5100 nM, respectively, for DDH.

For comparison, the 'base-on' analogue HO–Cbl proved to be the strongest inhibitor with K_i values slightly lower than the K_m for coenzyme B_{12} (Ado–Cbl), while CN–Cbl was about as potent as the poorest hydroxyalkyl-Cbl (*Table 4*). Finally, the parent 'base-off' corrinato complex HO–PTC, bearing a β-hydroxo ligand, showed only very weak or no detectable inhibition in the GDH or DDH reactions, respectively.

Table 1. *500-MHz ^{1}H-NMR Chemical-Shift Data* (D_2O, pH 7.4, 10°) *for Coenzyme B_{12} (Ado–Cbl) and Hydroxyalkyl Derivatives* **1a**,**b** *and* **2a**,**b**[a]). Chemical shifts relative to TSP (=sodium 3-(trimethylsilyl) (D_4)propanoate).

	Signal type	Chemical shifts [ppm]				
		Ado–Cbl[b])	[(*R*)-(HO)$_2$pr]–Cbl (**2b**)	[(*S*)-(HO)$_2$pr]–Cbl (**2a**)	HO(CH$_2$)$_3$–Cbl (**1b**)	HO(CH$_2$)$_2$–Cbl (**1a**)
Corrin Me						
Me–C(1)(a)	br. *s*	0.47	0.537	0.454	0.540	0.510
Me–C(2)(e)	br. *s*	1.36	1.420	1.382	1.411	1.409
Me–C(5)	*s*	2.45[c])	2.514	2.519	2.524	2.537
Me–C(7)(e)	br. *s*	1.70	1.798	1.864	1.805	1.823
Me$_\alpha$–C(12)(e)	br. *s*	1.32	1.443	1.398	1.468	1.458
Me$_\beta$–C(12)(a)	br. *s*	0.87	1.178	1.260	1.115	1.143
Me–C(15)	br. *s*	2.43	2.506	2.523	2.504	2.512
Me–C(17)(a)	*s*	1.36	1.466	1.441	1.426	1.430
Corrin CH						
H–C(3)(e)	*dd*	4.10	4.070	4.066	4.076	4.101
H–C(8)(e)	*dd*	3.29	3.401	3.278	3.403	3.403
H–C(10)	*s*	5.93	6.059	6.045	6.072	6.069
H–C(13)(e)	*dd*	2.89	3.238	3.248	3.240	3.260
H–C(18)(a)	*ddd*	2.65	2.67	2.67	2.68	2.672
H–C(19)(a)	*d*	4.24	4.638	4.183	4.157	4.138
Corrin CH$_2$						
CH$_2$(2^1)$_{a,b}$	*d*	2.41	2.582, 2.381	2.422, 2.378	2.43, 2.42	2.452, 2.389
CH$_2$(3^1)$_{a,b}$	*m*	2.06, 1.96	2.154, 2.025	2.103, 1.970	2.135, 2.030	2.120, 2.015
CH$_2$(3^2)$_{a,b}$	*ddd*	2.50	2.56, 2.486	2.535, 2.460	2.55, 2.48	2.55, 2.48
CH$_2$(7^1)$_{a,b}$	*d*	2.19, 1.72	2.547, 1.976	2.452, 2.232	2.5375, 2.023	2.550, 2.031
CH$_2$(8^1)$_{a,b}$	*m*	1.75, 0.81	1.815, 0.805	1.895, 0.950	1.84, 0.830	1.860, 0.845
CH$_2$(8^2)$_{a,b}$	*ddd*	1.73, 0.88	1.815, 0.908	1.83, 0.910	1.80, 0.970	1.82, 0.954
CH$_2$(13^1)$_{a,b}$	*m*	2.22, 2.00	2.16, 2.11	2.22, 2.145	2.115, 2.08	2.10, 2.07
CH$_2$(13^2)$_{a,b}$	*ddd*	2.54	2.64, 2.61	2.65, 2.62	2.65, 2.625	2.65, 2.63
CH$_2$(17^1)$_{a,b}$ [d])	*ddd*	1.78	2.545, 1.836	2.555, 1.825	2.543, 1.830	2.552, 1.820
CH$_2$(17^2)$_{a,b}$ [d])	*ddd*	2.45, 2.06	2.477, 2.115	2.49, 2.120	2.47, 2.117	2.47, 2.10
CH$_2$(18^1)$_{a,b}$	*dd*	2.65	2.751, 2.662	2.751, 2.655	2.767, 2.68	2.769, 2.675
1-Aminopropan-2-ol						
CH$_2$(1)(Apr)$_{a,b}$	*dd*	3.54, 3.16	3.538, 3.213	3.553, 3.191	3.540, 3.204	3.547, 3.168
CH(2)(Apr)	*dddq*	4.33	4.354	4.345	4.355	4.345
Me(3)(Apr)	*d*	1.21	1.207	1.215	1.209	1.214
*Loop ribose (*C(3′)*-endo)*						
H$_\alpha$–C(1′)(Rib)	*d*	6.26	6.285	6.294	6.279	6.287
H–C(2′)(Rib)(e)	*dd*	4.23	4.241	4.236	4.241	4.235
H–C(3′)(Rib)(a)	*dd*	4.72	4.753	4.756	4.748	4.743
H–C(4′)(Rib)(a)	*dddd*	4.10	4.131	4.116	4.132	4.117
CH$_2$(5′)(Rib)$_{ab}$(*g*,*g*)	*dd*	3.88, 3.74	3.913, 3.755	3.914, 3.754	3.915, 3.755	3.915, 3.751
Dimethylbenzimidazol						
H–C(2)(Dbi)	*s*	6.95	6.989	6.983	6.989	6.969
H–C(4)(Dbi)	br. *s*	6.24	6.252	6.282	6.269	6.289
H–C(7)(Dbi)	br. *s*	7.16	7.189	7.197	7.186	7.195
Me–C(5)(Dbi)	*s*	2.19	2.242	2.242	2.244	2.248
Me–C(6)(Dbi)	*s*	2.19	2.230	2.234	2.233	2.236
Alkyl-Co						
CH$_2$(1″)$_{a,b}$	*dd*(*d*)	1.55, 0.57[e])	1.118, 0.507	1.589, 0.843	1.375, 0.535	1.361, 0.597
H–C(2″) or CH$_2$(2″)$_{a,b}$	*m*	2.54[e])	1.681	1.647	0.50, −0.13	2.54, 1.960
CH$_2$(3″)$_{a,b}$	*dd*(*d*)		2.885, 2.778	2.836, 2.730	3.10, 3.07	

[a]) Numbering scheme according to the *Figure*; configuration codes in parentheses: a = axial, e = equatorial, *t* = *trans*, *g* = *gauche*, superscripts 1 or 2 refer to positions in corrin side chains; subscripts a and b refer to the high-frequency and low-frequency proton of CH_2 groups; Apr = 1-aminopropan-2-ol, Dbi = 5,6-dimethyl-1*H*-benzimidazole, Ade = adenine, Tol = *p*-tolyl; Rib and Ade–Rib refer to loop ribose (α-side) and adenosyl ribose (β-side), resp. All assignments were confirmed by COSY and NOESY data, with the exception (see *Footnote d*) of the assignments for CH$_2$(17^1) and CH$_2$(17^2) which may be reversed (coupling or NOE with Me–C(17) not detected). [b]) From [30], pH 7.0, 20°. [c]) Cited as 1.45 (typographical error) in [16] and [29]; in [29], the shift for Me–C(5) of compound **1a** should be 2.439 ppm. [d]) The original assignments for CH$_2$(17^1) and CH$_2$(17^2) in Ado–Cbl [30] are given here as corrected (reversed) by *Pagano et al.* [31]; our assignments are made by analogy, considering the H–C(17^1)$_b$ and H–C(17^2)$_b$ shifts; our previous assignments for AdoO(CH$_2$)$_n$–Cbl derivatives [29] should also be reversed. [e]) For Ado–Cbl, CH$_2$(1″)$_{a,b}$ correspond to CH$_2$(5′)(Ade–Rib)$_{a,b}$ and H–C(2″) to H–C(4′)(Ade–Rib).

Table 2. *500-MHz ^{1}H-NMR Chemical-Shift Data* (D_2O, pH 7.4, 10°) *for 'Base-off' Coenzyme B_{12}* ('base-off' form of Ado–Cbl) *and (Coβ-X)–PTC Derivatives* **3a**,**b** [a]). Chemical shifts relative to TSP (=sodium 3-(trimethylsilyl) (D_4)propanoate).

	Signal type	Chemical shifts [ppm]			
		Ado–'Cbl' ('base-off') [b])	Ado–PTC [c])	[(*R*)-(HO)$_2$pr]–PTC (**3b**)	[(*S*)-(HO)$_2$pr]–PTC (**3a**)
Corrin Me					
Me–C(1) (a)	br. *s*	0.81	0.704	0.788	0.786
Me–C(2) (e)	br. *s*	1.48	1.405	1.511	1.469
Me–C(5)	*s*	2.43	2.389	2.374	2.399
Me–C(7) (e)	br. *s*	1.82	1.819	1.854	1.923
Me$_\alpha$–C(12) (e)	br. *s*	1.67	1.585	1.648	1.640
Me$_\beta$–C(12) (a)	br. *s*	1.00	0.845	1.037	1.094
Me–C(15)	br. *s*	2.46	2.336	2.483	2.484
Me–C(17) (a)	*s*	1.40	1.141	1.498	1.469
Corrin CH					
H–C(3) (e)	*dd*	4.23	4.217	4.047	4.128
H–C(8) (e)	*dd*	3.73	3.784	3.797	3.797
H–C(10)	*s*	6.97	6.994	7.025	7.036
H–C(13) (e)	*dd*	3.43	3.308	3.543	3.557
H–C(18) (a)	*ddd*	2.85	2.787	2.870	2.906
H–C(19) (a)	*d*	4.70	4.653	5.106	4.733
Corrin CH$_2$					
CH$_2$(2^1)$_{a,b}$	*d*	2.60, 2.46	2.66, 2.285	2.665, 2.495	2.599, 2.480
CH$_2$(3^1)$_{a,b}$	*m*	2.11, 1.97	1.99, 1.89	2.05, 1.925	2.012, 1.91
CH$_2$(3^2)$_{a,b}$	*ddd*	2.55	2.507, 2.475	2.532, 2.49	2.520, 2.50
CH$_2$(7^1)$_{a,b}$	*d*	2.61, 2.14	2.275, 1.731	2.440, 1.983	2.460, 2.130
CH$_2$(8^1)$_{a,b}$	*m*	2.21, 1.75	2.250, 1.81	2.295, 1.835	2.32, 1.88
CH$_2$(8^2)$_{a,b}$	*ddd*	2.35, 2.35	2.41, 2.31	2.445, 2.36	2.43, 2.315
CH$_2$(13^1)$_{a,b}$	*m*	2.21, 1.92	2.185, 1.885	2.25, 1.960	2.24, 1.95
CH$_2$(13^2)$_{a,b}$	*ddd*	2.21, 1.86	2.148, 1.788	2.185, 1.830	2.174, 1.809
CH$_2$(17^1)$_{a,b}$ [d])	*ddd*	2.51, 1.85	2.425, 1.76	2.525, 1.835	2.55, 1.86
CH$_2$(17^2)$_{a,b}$ [d])	*ddd*	2.31, 1.85	2.365, 1.833	2.39, 1.86	2.45, 1.86
CH$_2$(18^1)$_{a,b}$	*dd*	2.78	2.68, 2.49	2.823	2.85, 2.80
1-Aminopropan-2-ol (Apr)					
CH$_2$(1)(Apr)$_{a,b}$	*dd*	3.38, 3.27	3.470, 3.395	3.45, 3.42	3.475, 3.426
CH$_2$(Apr)	*dddq*	4.36	4.42	4.416	4.423
Me(3)(Apr)	*d*	1.23	1.238	1.248	1.255
Loop ribose (C(2′)-*endo*)					
H$_\alpha$–C(1′)(Rib) (e)	*d*	6.56	5.664	5.660	5.670
H–C(2′)(Rib) (a)	*dd*	4.97	4.331	4.333	4.339
H–C(3′)(Rib) (e)	*dd*	4.83	4.551	4.550	4.557
H–C(4′)(Rib) (a)	*dd*	4.79	4.38	4.389	4.398
CH$_2$(5′)(Rib)$_{a,b}$(*g*,*g*)	*dd*	3.94, 3.84	3.72, 3.70	3.71, 3.70	3.725, 3.710
Tolyl					
H–C(2)/H–C(6)(Tol)	*d*		6.873	6.878	6.890
H–C(3)/H–C(5)(Tol)	*d*		7.026	7.033	7.044
Me–C(4)(Tol)	*s*		2.128	2.120	2.136
Adenosyl					
H–C(2)(Ade)	*s*	8.43	8.234		
H–C(8)(Ade)	*s*	8.21	8.037		
H$_\beta$–C(1′)(Ade–Rib)	*d*	5.61	5.615		
H–C(2′)(Ade–Rib) (e)	*dd*	4.34	4.40		
H–C(3′)(Ade–Rib) (a)	*dd*	3.90	3.754		
H–C(4′)(Ade–Rib) (a)	*ddd*	1.98	2.002		
CH$_2$(5′)(Ade–Rib)$_{a,b}$(*g*,*t*)	*dd*	1.46, 0.38	0.602, 0.312		
Dihydroxypropyl					
CH$_2$(1″)$_{a,b}$(*t*,*g*)	*dd*			0.953, –0.134	1.064, 0.372
H–C(2″)	*m*			1.04	1.006
CH$_2$(3″)$_{a,b}$(*t*,g)	*dd*			2.712, 2.642	2.670, 2.534

[a]) See *Footnote a* in *Table 1*. [b]) From [32], pH 2.1. [c]) From [29], with minor revisions for some of the corrin CH$_2$ groups. [d]) Our assignments for CH$_2$(17^1) and CH$_2$(17^2) are not definitive (NOEs with Me–C(17) not detected) but are made by analogy with those for 'base-off' Ado–'Cbl'.

Table 3. *$^1H,^1H$-Coupling Constants* J [Hz] *for Ribose Moieties or Hydroxyalkyl Chains in Coβ-X Derivatives*

	J[Hz][a])	
Ado–Cbl[b])	Ade–Rib	$^2J(5'a,5'b) = -9.2$, $^3J(4',5'a) = <2$, $^3J(4',5'b) = 9.2$, $^3J(3',4') = 6.7$, $^3J(2',3') = 5.8$, $^3J(1',2') = 3.3$
	loop Rib	$^2J(5'a,5'b) = -13.0$, $^3J(4',5'a) = 2.7$, $^3J(4',5'b) = 3.9$, $^3J(3',4') = 8.9$, $^3J(2',3') = 4.3$, $^3J(1',2') = 3.0$
Ado–PTC	Ade–Rib	$^2J(5'a,5'b) = -8.5$, $^3J(4',5'a) = 1.0$, $^3J(4',5'b) = 9.0$, $^3J(3',4') = 6.2$, $^3J(2',3') = 6.2$, $^3J(1',2') = 3.8$
	loop Rib	$^2J(5'a,5'b) = -13.0$, $^3J(4',5'a) = 3.0$, $^3J(4',5'b) = 3.5$, $^3J(3',4') = 2.5$, $^3J(2',3') = 6.3$, $^3J(1',2') = 4.6$
[(*R*)-(HO)$_2$pr]–Cbl (**2b**)		$^2J(1a,1b) = -9.5$, $^3J(1a,2) = 6.9$, $^3J(1b,2) = 1.8$, $^3J(2,3a) = 7.3$, $^3J(2,3b) = 4.8$, $^2J(3a,3b) = -11.4$
[(*R*)-(HO)$_2$pr]–PTC (**3b**)		$^2J(1a,1b) = -7.7$, $^3J(1a,2) = 7.7$, $^3J(1b,2) = 1.0$, $^3J(2,3a) = 6.5$, $^3J(2,3b) = 5.6$, $^2J(3a,3b) = -11.4$
[(*S*)-(HO)$_2$pr]–Cbl (**2a**)		$^2J(1a,1b) = -8.9$, $^3J(1a,2) = 5.5$, $^3J(1b,2) = 4.2$, $^3J(2,3a) = 6.9$, $^3J(2,3b) = 4.1$, $^2J(3a,3b) = -11.4$
[(*S*)-(HO)$_2$pr]–PTC (**3a**)		$^2J(1a,1b) = -7.5$, $^3J(1a,2) = 4.0$, $^3J(1b,2) = 5.3$, $^3J(2,3a) = 6.9$, $^3J(2,3b) = 4.9$, $^2J(3a,3b) = -11.4$
HO(CH$_2$)$_3$–Cbl (**1b**)[c])		$^3J(2,3a) = 6.9$ and 6.3, $^3J(2,3b) = 6.4$ and 4.2, $^2J(3a,3b) = -10.7$
HO(CH$_2$)$_2$–Cbl (**1a**)[c])		$^2J(1a,1b) = -7.0$, $^3J(1a,2a) = 6.0$, $^3J(1a,2b) = 12.6$, $^3J(1b,2a) = 12.5$, $^3J(1b,2b) = 4.8$, $^2J(2a,2b) = -10.5$

[a]) Alkyl atoms C(1), C(2), and C(3) (″ symbol omitted) are numbered starting with the Co-bound atoms and correspond to adenosyl C-atoms C(5′), C(4′), C(3′). [b]) From [30]. [c]) Tentative assignments; complete determination of all coupling constants was not possible.

Table 4. *Kinetic Properties of Hydroxyalkyl Derivatives* **1a–d** *and* **2a**,**b** ((*Coβ*-X)–Cbl) *and* **3a**,**b** ((Coβ-X)–PTC) *with Glycerol Dehydratase and Diol Dehydratase*

	K_i [nM][a])		Relative ΔG [kJ/mol][d])	
Inhibitor	GDH[b])	DDH[c])	GDH[b])	DDH[c])
HO–Cbl[e])	8.6 ± 1.4	680 ± 110	−0.98	−0.15
Ado–Cbl (K_m data)	12.6 ± 2.2	720 ± 80	0.0	0.0
HO(CH$_2$)$_2$–Cbl (**1a**)	13.4 ± 3.2	770 ± 70	0.16	0.17
HO(CH$_2$)$_3$–Cbl (**1b**)	13.3 ± 3.1	760 ± 70	0.14	0.14
[(*S*)-(HO)$_2$pr]–Cbl (**2a**)	14.8 ± 4.1	1080 ± 100	0.41	1.04
[(*R*)-(HO)$_2$pr]–Cbl (**2b**)	17.6 ± 4.8	1250 ± 110	0.86	1.42
HO(CH$_2$)$_4$–Cbl (**1c**)	17.0 ± 4.5	1060 ± 90	0.77	0.99
HO(CH$_2$)$_5$–Cbl (**1d**)	25.2 ± 7.8	950 ± 80	1.78	0.71
CN–Cbl[e])	21.6 ± 2.7	1420 ± 200	1.38	1.74
[(*S*)-(HO)$_2$pr]–PTC (**3a**)	57 ± 7	5100 ± 490	3.87	5.02
[(*R*)-(HO)$_2$pr]–PTC (**3b**)	348 ± 31	6400 ± 580	8.52	5.61
Ado–PTC	160 ± 37	9200 ± 1700	6.52	6.54
HO–PTC	9960 ± 100	> 25000[f])	17.13	> 9.1

[a]) Apparent inhibition constants at 37°, estimated by the 'parallel' method [41]; apparent K_m constants for Ado–Cbl were measured as described previously [26][41]. [b]) Glycerol dehydratase from overexpressing *Escherichia coli* containing the gene from *Citrobacter freundii* ($V_{max} = 48 \pm 4$ nmol/min with Ado–Cbl). [c]) Diol dehydratase from overexpressing *Escherichia coli* containing the gene from *Salmonella typhimurium* ($V_{max} = 51 \pm 6$ nmol/min with Ado–Cbl). [e]) From [16]. [f]) No significant inhibition was found for up to 25 μM HO–PTC. [d]) Estimated free energy of inhibitor binding relative to Ado–Cbl; calculated as $RT \ln(K_i/K_m)$ at 37°.

Discussion. – *Structural Properties of the Coenzyme-B_{12} Analogues.* Molecular-modeling studies for Ado–Cbl and the [(*R*)- and (*S*)–(HO)$_2$pr]–Cbl (**2a**,**b**) gave low-energy conformations which faithfully reproduced the geometries of the crystal structures, including the non-planar characteristics of the corrin ring, the axial/equatorial orientation of side chains, the loop and ribose conformations, and the orientations of adenosyl and dimethylbenzimidazole (Dbi) groups. These features are accurately represented in the diagrams of the *Figure*. It should be noted, however, that

good agreement between modeled and crystal structures was only obtained after adding appropriate parameters to the HyperChem force field for bonds to the Co- and P-atom.

The dihedral angles for protons in the adenosyl ribose (Ade–Rib) of Ado–Cbl in the crystal structure differed by $<20°$ from those in the energy-minimized modeled structure. The C(3′)-*endo* ribose conformation (H–C(3′) axial) in the crystal must predominate in solution for both Ado–Cbl and Ado–PTC since the observed vicinal coupling constants $J(1',2')$, $J(2',3')$, and $J(3',4')$ were 3.3, 5.8, and 6.7 Hz for Ado–Cbl [30] and 3.8, 6.2, 6.2 Hz for Ado–PTC [16], consistent with the modeled torsional angles of *ca.* 105, 38, and $-168°$ obtained for Ado–Cbl. The modeled torsional angles for the C(4′)–C(5′) bond in Ado–Cbl were 69 and $-174°$, consistent with $J(4',5'a)$ and $J(4',5'b)$ of <2 and 9.2 Hz, respectively, in Ado–Cbl and 1.0 and 9.0 Hz, respectively, in Ado–PTC. Thus, H_b–C(5) is *trans* to H–C(4′) and oriented towards the corrin C(10) atom while H_a–C(5′) points toward the corrin-ring A. These orientations result in a *ca.* 1-ppm upfield shift for H_b–C(5′) relative to H_a–C(5′) in both Ado–Cbl and Ado–PTC. The ribose ring lies nearly perpendicular to the corrin ring with the ribose-ring O-atom pointing towards the corrin C(14) atom. The adenine ring is in the *syn* conformation, nearly parallel to the corrin ring and positioned over the corrin-ring C. This results in the characteristic upfield shift of *ca.* 0.3 ppm for Me_β–C(12) of the Ado derivatives relative to the hydroxyalkyl derivatives.

In the nucleotide loop of the Cbl derivatives, the α-ribose conformation is also C(3′)-*endo* (dihedral angles of $-26°$ for protons H–C(1′), H–C(2′), $40°$ for H–C(2′), H–C(3′), and $-167°$ for H–C(3′), H–C(4′)), resulting in a coupling-constant pattern similar to that for the Ade–Rib. The predominance of the C(4′)–C(5′) rotamer with OH *trans* and both H–C(5′) *gauche* to H–C(4′) is confirmed by the small values of both coupling constants. In PTC derivatives, the nucleotide loop is open and flexible. In this case the loop ribose adopts predominantly a C(2′)-*endo* (H–C(2′) axial) conformation (dihedral angles of $42°$ for H–C(1′), H–C(2′), $-37°$ for H–C(2′), H–C(3′), and $-106°$ for H–C(3′), H–C(4′) result in vicinal coupling constants of 4.6, 6.3, and 2.5 Hz, resp.). Modeling indicates that the C(2′)-*endo* and C(3′)-*endo* ribose conformations have only a small energy difference (<4 kJ/mol) for an open nucleotide loop, but that the C(3′)-*endo* conformer is preferred when the loop is closed and Dbi is attached to the Co-atom.

The loss of the Dbi group as α-ligand at the Co-atom perpendicular to the corrin plane in the 'base-off' derivatives removes Dbi as a source of upfield aromatic-ring shift effects. Therefore, corrin groups pointing downwards and normally oriented over the plane of Dbi (*i.e.*, Me–C(1), Me–C(2), Me_α–C(12), $CH_2(8^1)$, and $CH_2(8^2)$) move downfield in the 'base-off' analogues. In the modeling studies, it was found that the cobalamin conformational energy is lowered by several kJ/mol when the side chain located at C(8) and pointing axially downwards is oriented to place the CH_2 groups very close to the face of Dbi (hydrophobic stabilization); this intramolecular interaction is responsible for the unique and abnormally large shielding of these CH_2 groups relative to other side chains. This effect is lost in the PTC derivatives. In addition, all of the corrin-ring protons are shifted downfield in the PTC analogues (by as much as 1 ppm for H–C(10); this probably reflects a significant change in electron density at the Co-atom (and the corrin ring system) in the 'base-off' form.

Some interesting conformational properties of the hydroxyalkyl ligands in the coenzyme-B_{12} analogues discussed here can be derived from the analysis of chemical shifts and couplings. The crystal structure of [(*R*)-$(HO)_2$pr−Cbl (**2b**) [28] shows that the Co−C(1″) bond has the same angular orientation as the Co−C(5′) bond in Ado−Cbl with the *pro-S* proton (H_a−C(1″) or H_a−C(5′)) pointing towards the corrin-ring A and the *pro-R* proton (H_b−C(1″) or H_b−C(5′)) pointing toward C(10). In contrast, C(1″) is rotated by *ca.* 90° counterclockwise in the (*S*)-$(HO)_2$pr derivative **2a** so that H_{Si}−C(1″) points towards H−C(19) and H_{Re}−C(1″) towards Me−C(5). Here, we distinguish CH_2 protons by the subscripts a and b to denote low- and high-field shifts (high and low frequencies), respectively, and *Re* and *Si* to designate the *pro-R* and *pro-S* positions. This conformational difference between the two dihydroxypropyl derivatives (confirmed as energy minima in modeling studies) is reflected in the chemical shifts of the CH_2(1″) protons. For [(*R*)-$(HO)_2$pr]−Cbl (**2b**) H_b−C(1″) has nearly the same strongly shielded chemical shift as H_b−C(5′) in Ado−Cbl (*pro-R* position) while H_a−C(1″) (H_a−C(5)) resonates downfield by 0.61 (0.98) ppm (*pro-S* position). For [(*S*)-$(HO)_2$pr]−Cbl (**2a**), both chemical shifts are less shielded by *ca.* 0.4 ppm, consistent with a rotation away from the central part of the delocalized corrin double-bond system. This trend is also observed for the $(HO)_2$pr−PTC analogues, although there is a general increase in the local shielding effects when the Co-atom is in the 'base-off' form.

Another diagnostic feature is the chemical shift of the corrin H−C(19) which is shifted downfield by *ca.* 0.4 ppm in the (*R*)-$(HO)_2$pr *vs.* the (*S*)-$(HO)_2$pr or Ado derivative for both the Cbl and PTC analogues. The crystal structure shows that for [(*R*)-$(HO)_2$pr]−Cbl (**2b**), the O-atom of OH−C(2″) is relatively close to H−C(19) (2.6 Å) and is probably the source of the downfield shift [27]. This conformation corresponds to the lowest-energy C(1″)−C(2″) rotamer in the modeling studies (shown in the *Figure*); C(3″) is *trans* to Co and H−C(2″) is approximately *trans* to H_{Si}−C(1″) (*ca.* 145°) and at an angle of near −100° to H_{Re}−C(1″), consistent with the observed vicinal coupling constants for **2b** (*Table 3*; $J(1''a,2'') = 6.9$ and $J(1''b,2'') = 1.8$ Hz). Similar coupling constants are observed for [(*R*)-$(HO)_2$pr]−PTC (**3b**). On the other hand, the C(2″)−C(3″) bond is nearly vertical relative to the corrin plane, so that all three rotamers for the orientation of OH−C(3″) are possible. Thus, the difference between the two $J(2'',3'')$ in the (*R*)-$(HO)_2$pr derivatives is smaller.

In contrast, for [(*S*)-$(HO)_2$pr]−Cbl (**2a**), H_{Si}−C(1″) points towards H−C(19). Modeling indicates that two C(1″)−C(2″) rotamers are probably populated. One of these has OH−C(2″) *trans* to the Co-atom, as in the crystal structure, while the other has C(3″) *trans*, as shown in the *Figure*. Thus, each H−C(1″) may spend time in either a *trans* or a *gauche* position relative to H−C(2″), consistent with the observed $J(1'',2'')$ of 4–5 Hz. In the crystal structure, OH−C(3″) is *gauche* to OH−C(2″) and oriented towards Me−C(17), corresponding to the rotamer with H−C(2″) *gauche* to both H−C(3″). For the other C(1″)−C(2″) rotamer (C(3″) *trans* to Co), all three C(2″)−C(3″) rotamers should be possible, but the conformation with *trans*-OH groups and H_{Re}−C(3″) *trans* to H−C(2″) (*Figure*) may be favored, resulting in a larger coupling constant for H−C(2″) to H_{Re}−C(3″) (tentatively assigned as H_a−C(3″)). These observations and arguments apply to [(*S*)-$(HO)_2$pr]−PTC (**3a**) as well.

Another interesting feature of the spectra is the geminal coupling of the CH_2 group attached to the Co-atom. The magnitude of this coupling constant in the Ado– and $(HO)_2$pr–Cbl analogues ranges from 8.9 to 9.5 Hz but is reduced to 7.5 to 8.5 Hz in the corresponding PTC derivatives and to 7.0 for $HO(CH_2)_2$–Cbl (**1a**). A reduction in this coupling constant is consistent with an increase in the electron-withdrawing power of the Co-atom in its 'base-off' form or of OH–C(2″) when the C(3″) atom is absent. For $HO(CH_2)_2$–Cbl (**1a**), large *trans* vicinal coupling constants (12.5 Hz) were observed (J(1″a,2″b) and J(1″b,2″a)). This indicates that the hydroxyethyl group adopts exclusively a staggered conformation with Co and OH in a *trans* ('*anti*') relationship and with H_a–C(1″) and H_a–C(2″) pointing toward the 'west' side of the corrin ring and the more strongly shielded H_b–C(1″) and H_b–C(2″) pointing toward the 'east'. For $HO(CH_2)_3$–Cbl (**1b**), a detailed analysis of the alkyl coupling constants could not be made, but the CH_2(1″) chemical shifts and the shift difference for CH_2(2″) were very similar to the values observed for $HO(CH_2)_2$–Cbl (**1a**), indicating similar conformational properties.

In summary, we find that the upper (β) and lower (α) regions of the corrin ring system in coenzyme-B_{12} analogues are largely independent in their conformational properties. The β-ligands (Ado, hydroxyalkyl) behave the same in the 'base-on' Cbl and 'base-off' PTC derivatives. These ligands are restricted in their conformational freedom by the various Me groups and side chains at the corrin ring. The crystal structures of Ado–Cbl and the $(HO)_2$pr derivatives appear to provide good representations for the (predominant) conformation in solution. It is interesting to note that C(4′) of the adenosyl ligand has the same (S)-configuration as C(2″) of the (S)-$(HO)_2$pr derivative (*Fig.*). Surprisingly, the (S)-$(HO)_2$pr derivative has a significantly different conformation and orientation of the C_3 chain compared to the Ado (C(3′)–C(4′)–C(5′)) and (R)-$(HO)_2$pr ligands, which show highly similar conformations. However, in the modeled structures, the orientations of the OH groups of the (R)-$(HO)_2$pr derivative poorly match those of Ado, while OH–C(3″) of the (S)-$(HO)_2$pr derivative and OH–C(2′) of Ado both point toward the corrin-ring D and are located 4.5–5 Å above the corrin C(16) atom. Thus, the (S)-$(HO)_2$pr derivative may interact more favorably than the (R)-form with a putative ribose binding site or with a substrate binding site (see below), resulting in the observed difference between the inhibition constants K_i.

Inhibitor Properties of the Coenzyme-B_{12} Analogues. From the data in *Table 4*, we note that the absolute values of K_i of inhibitors and K_m of coenzyme B_{12} differ by a factor of 20 or more for glycerol dehydratase and for diol dehydratase. However, there are crude similarities in the order or ranking of inhibitor potencies (relative K_i values) for the two enzymes. Such a similarity may be a result of the homology found in the amino-acid sequences of several representatives of these two kinds of dehydratases [24][25]. Furthermore, both dehydratases accept either glycerol or racemic propane-1,2-diol as substrate [29][33].

As expected, all of the 'base-on' hydroxyalkyl analogues were efficient inhibitors of both enzymes with a narrow range of apparent K_i. The K_i values differed by, at most, a factor of two from the apparent K_m for coenzyme B_{12} (Ado–Cbl). It should be noted that such a range of K_i corresponds to differences in a binding free energy $\Delta G = \Delta H - T\Delta S$ of less than 2 kJ/mol, which is less than the ΔG associated with a single H-bond

(*ca.* 5 kJ/mol), and certainly within the range of possible variations due to entropy effects alone [34]. For both enzymes, the two short-chain monohydroxy analogues **1a**,**b**, *i.e.* $OH(CH_2)_n$–Cbl ($n = 2$ and 3), had lower K_i relative to the long-chain derivatives **1c**,**d** ($n = 4$ and 5). One possible interpretation of this result is that a hydrophilic area of interaction between the β-ligand and the protein must lie relatively close to the Co-center. However, when one compares ligands with different chain lengths and, therefore, different degrees of freedom for internal motions, the loss of motional entropy upon binding to a protein must be taken into account. At room temperature, this effect on ΔG for binding has been estimated to be *ca.* + 1.4 kJ/mol for each single bond whose motion is 'frozen' in the complex [34]. Thus, for alkyl groups with two to five C-atoms, interaction of a terminal OH group with a binding pocket in the protein is expected to result in an entropy penalty which increases with chain length and which may compensate for or even exceed any negative enthalpy changes due to increasing hydrophobic interactions with increasing alkyl chain length, for example.

The kinetic results obtained with the 'base-on' dihydroxypropyl analogues **2a**,**b** indicate that a second OH group in the β-ligand provides no significant increase in binding affinity. This is consistent with the hypothesis that the ligand interacts with the substrate binding site and that only the terminal (primary) OH group of the substrate (or ligand) can be involved in binding (see *Introduction*). Alternatively, the β-ligand may interact with a ribose binding site which is possibly utilized by the natural coenzyme. Theoretically, two ribose OH groups are available for H-bonding, but our NMR and modeling studies indicate that in the favored conformations of the dihydroxypropyl ligands, only one OH group can adopt an orientation similar to the adenosyl OH–C(2′), for example. This 'match' in orientation was better for the [(*S*)-$(HO)_2$pr]–Cbl (**2a**), and this analogue was indeed a slightly better inhibitor compared to the [(*R*)-$(HO)_2$pr]–Cbl (**2b**). However, the monohydroxyalkyl ligands may have a small advantage of greater conformational flexibility for positioning the terminal OH group in the appropriate orientation for binding.

It is interesting and perhaps surprising to note that the simple hydroxyethyl and hydroxypropyl groups as β-ligands in **1a**,**b** result in inhibitors with K_i equal to the K_m for coenzyme B_{12} (Ado–Cbl). One possible explanation is that the binding stabilization provided by the adenosyl moiety is simply limited to the interaction of a single OH group with the protein, an interaction which can be generated also by the small hydroxyalkyl group. Another and perhaps more likely explanation is that the bulky adenosyl group introduces positive contributions to ΔG (steric repulsions, 'induced fit' energy, *etc.*) which largely compensate the available negative, stabilizing contributions. In general, however, it is quite difficult to describe binding interactions and to interpret the small differences in *Table 4* in an *a priori* manner without knowledge of binding-site geometry and the residues involved (X-ray structures are not available for the enzymes discussed here). A further difficulty arises when binding *via* H-bonds is concerned. Not only the number of putative H-bonds in the complex is important, but also the net change in the total number of H-bonds after complexation and the net change in the number of free solvent H_2O molecules. For all of the Cbl derivatives presented here, the small range of ΔG values represents small differences in the sums over a series of much larger numbers (enthalpies and entropies with positive and negative contributions). The differences in ΔG are smaller than the free energy we can assign to any single

discrete interaction such as one H-bond. Thus, it is probably reasonable to consider all Cbl derivatives examined here as *essentially* equally good inhibitors for GDH and DDH.

In contrast, the 'base-off' PTC analogues **3a**,**b** are significantly poorer inhibitors and exhibit a much wider range of potencies and larger differences in relative K_i values for the two enzymes. One expects that the 'unattached' nucleotide loop at the PTC derivatives can, in principle, be folded so as to fit into the presumed binding pocket utilized by the natural coenzyme and its Cbl analogues [16]. Thus, essentially the same enthalpy of binding should be achievable for Ado–PTC as for Ado–Cbl, but this requires a significant entropy penalty since several degrees of freedom in the 'open' loop will be reduced, if not frozen, in the final 'closed' or 'base-on' conformation upon binding. As many as ten single bonds are involved whose mobilities will be reduced in the complex. For an entropic contribution of 1.4 kJ/mol per bond, one predicts an increase in ΔG of up to 14 kJ/mol, which covers the range of 4–8 kJ/mol calculated for Ado–PTC and the dihydroxypropyl derivatives **3a**,**b** (*Table 4*). The differences *between* these three inhibitors are larger than for the Cbl analogues, but still no larger than the free-energy contribution for a single H-bond. As observed for the Cbl derivatives, the [(*S*)-(HO)$_2$pr]–PTC (**3a**) is a better inhibitor than the (*R*)-isomer **3b**; it is, in fact, even better than the Ado analogue. This is consistent with the concept that the small (*S*)-(HO)$_2$pr ligand can enter into favorable interactions with either a substrate or ribose site. These interactions may be similar to those pursued by the Ado ligand, but perhaps without unfavorable compensating effects (*e.g.*, protein conformational changes) caused by the adenosyl's bulk, which may be more important when a closed nucleotide loop is not already present.

It is surprising that HO–PTC itself (with a β-hydroxo ligand) proved to be a very poor inhibitor, while the analogue HO–Cbl is the best inhibitor. This is clearly not explainable with simple entropy effects. One possibility is that the binding of coenzyme-B$_{12}$ analogues occurs in a stepwise manner and that stabilizing interactions between an appropriate β-ligand and the protein are first necessary to give the PTC nucleotide loop the opportunity to adequately fold to occupy the normal Dib-loop pocket. For HO–PTC, the initial complex may not be stable enough to promote this folding process or induction of the corresponding optimal protein conformation. For HO–Cbl the corrin moiety and the nucleotide loop presumably already have the optimal, relatively rigid conformation, so that binding can proceed directly without the need for a prestabilizing complex. As is well-known in drug design, if an inhibitor can be produced with a rigid conformation matching the bound or active conformation of an otherwise flexible substrate, then binding affinity may be enhanced by several orders of magnitude.

In conclusion, the inhibition kinetic data presented here confirm that both glycerol dehydratase and diol dehydratase reactions utilize the 'base-on' binding mode of coenzyme B$_{12}$. A series of 'base-on' cobalamin derivatives with hydroxyalkyl ligands on the β-side, *i.e.*, **1a**–**d** and **2a**,**b**, proved to be strong competitive inhibitors of the dehydratases with a narrow range of K_i; the best inhibitor had K_i equal to K_m of coenzyme B$_{12}$. The 'base-off' corrinato complexes (PTC analogues) with adenosyl or hydroxyalkyl ligands on the β-side, *i.e.*, **3a**,**b**, exhibited significant but poorer potency as inhibitors. The parent compound HO–PTC, with only a β-hydroxo ligand, was a very

poor inhibitor while HO–Cbl was the best for both enzymes. These results indicate that for the 'base-off' analogues interactions between the β-ligand and a hydrophilic binding site near the Co-center (for substrate or possibly for the adenosyl ribose) are important for stabilizing an initial complex and facilitating the folding of the nucleotide loop into a 'base-on' conformation in the final inhibitor-apoenzyme complex. All Cbl analogues have the 'ideal' 'base-on' conformation of the nucleotide loop, and their potencies as inhibitors, judged by K_i, are much less dependent upon the nature of the β-ligand.

Experimental Part

Materials. Coenzyme B_{12}, vitamin B_{12a} ω-haloalkanols, and sodium tetrahydroborate ($NaBH_4$) were obtained from *Fluka Chemie AG*. The enantiomeric (*R*)- and (*S*)-3-chloropropane-1,2-diols were obtained by enzymic resolution [35]. Racemic propane-1,2-diol was supplied by *Aldrich*. (Coα-Cyano)(Coβ-hydroxo) [1′-*O*-(*p*-tolyl)cobamide] (HO–PTC) was isolated from *Sporomusa ovata* cells by extraction with KCN-containing AcOH buffer at pH 5 followed by centrifugation, treatment of the supernatant by neutral aluminum oxide, desalting, chromatography on a *XAD-2* column, and reversed-phase HPLC (*RP18*) as previously described [36–38]. Yeast alcohol dehydrogenase and β-NADH Li_3 (NADH) were products of *Boehringer Mannheim GmbH*. Glycerol dehydratase (GDH) was isolated as described previously [26] from overexpressing *Escherichia coli* cells containing the genomic DNA for glycerol dehydratase from *Citrobacter freundii* [25][39]. Propanediol dehydratase (DDH) was isolated as reported previously [26] from overexpressing *E. coli* cells containing genes for diol dehydratase from *Salmonella typhimurium* LT2.

[(2-Hydroxyethyl)-, (3-Hydroxypropyl)-, (4-Hydroxybutyl)-, and (5-Hydroxypentyl)]cob(III)alamin (**1a**,**1b**,**1c**, and **1d**, resp.), *[(*S*)-2,3-Dihydroxypropyl]- and [(*R*)-2,3-Dihydroxypropyl]cob(III)alamin* (**2a** and **2b**, resp.), *and {Coβ-[(*S*)-2,3-Dihydroxypropyl]}- and {Coβ-[(*R*)-2,3-Dihydroxypropyl]}[1′-O-(p-tolyl)cobamide]* (**3a** and **3b**, resp.). To a soln. of HO–Cbl or HO–PTC (5 μmol) in deoxygenated H_2O (0.5 ml), a soln. of $NaBH_4$ (5 mg) in deoxygenated H_2O (0.4 ml) was added under Ar at r.t., and the resulting soln. was stirred for 30 min. Then a soln. of the corresponding ω-haloalkanol or -diol (50–100 μmol) in deoxygenated MeCN (0.4 ml) was added, and the mixture was stirred in the dark at r.t. for 1 h. After sterile filtration through a 30-kD nitrocellulose membrane, the mixture was submitted to prep. HPLC (*Macherey & Nagel*, 250 mm × 1″, *Nucleosil-7-C_{18}* column; 20–85% MeOH/H_2O gradient over 35 min, flow rate 5 ml/min; diode array detection, monitoring at 240 and 280 nm; UV spectra obtained between 200 and 600 nm from the HPLC peaks). The fractions containing the product were concentrated in a *SpeedVac* to give the desired (*Coβ*-X)–Cbl **1a**–**d** or **2a**,**b**, or (*Coβ*-X)–PTC **3a**,**b** in over 60% yields. Purities of the products were over 95% by anal. HPLC (*Macherey & Nagel*, 125 × 4 mm, 5 μm *LiChrospher 100 RP-18* column, linear gradient of 40–70% *B* in *A* over 12 min (*A:* 0.02% CF_3COOH in H_2O; *B:* 0.02% CF_3COOH in MeOH), flow rate 1 ml/min; diode-array detection).

^{1}H-NMR Spectroscopy. Solns. of (*Coβ*-X)–Cbl **1a**,**b** or **2a**,**b** (2.6–3.1 mg) or (*Coβ*-X)–PTC **3a**,**b** (0.7–0.9 mg) in 0.4 ml of a 20 mM sodium phosphate/D_2O buffer (pH-meter reading 7.4, 5-mm sample tube) were measured at 10° by means of a *Bruker-AM-500* spectrometer using conventional *Fourier* transform methods as in our previous studies [16][29]. The residual HDO resonance was suppressed by selective presaturation. Parameters for the 1D spectra of **1a**,**b** or **2a**,**b** were: spectral width 4310 Hz, 32 K time-domain points, presaturation for 3.1 s, 50° flip angle, acquisition time 3.8 s, 400 transients. Data processing was performed with zero-filling to 64 K data, *Lorentz-Gauss* resolution enhancement, and a digital resolution of 0.13 Hz. Similar parameters were used for **3a**,**b**. For well-resolved resonances, chemical shifts (given in three decimal places, rel. to internal sodium 3-(trimethylsilyl)propanoate (TSP)) and coupling constants were derived from the peak-picking output (cubic interpolation); chemical shifts, given in only two decimal places, were estimated from cross-peaks in the 2D COSY experiment. The total number of nonexchangeable protons was confirmed by integration, and the complete assignments are given in *Tables 1* and *2*.

Two-dimensional magnitude-mode COSY-β and NOESY data were obtained from conventional pulse sequences and the following parameters for **1a**,**b** or **2a**,**b**. COSY: spectral width 3906 Hz, 2 K time-domain points in t_2, acquisition time 0.261 s, 512 t_1 increments with 32 transients each, 40 ms initial delay in the t_1 time domain to enhance the effects of long-range couplings, $\beta = 50°$ as read pulse to improve the detection of cross-peaks close to the diagonal and provide some discrimination between vicinal and geminal couplings, relaxation delay with presaturation 2.25 s, sine-bell window functions, zero-filling to 1 K in t_1, digital resolution 3.8 Hz/pt.

NOESY: as for COSY, except 48 or 64 transients per t_1 increment, 90° read pulse, mixing time 500 ms with max. ±15% random variation. For **3a**,**b**, similar parameters were used except: presaturation delay 2.3 or 2.7 s, 30 ms initial t_1 delay for COSY, 600 ms mixing time for NOESY.

Molecular Modeling. As an aid to interpretation of the NMR data, modeling of Ado–Cbl and several of the analogues discussed here was performed using the MM+ force field of HyperChem 4.5 (*HyperCube*, *Inc.*), with additional parameters added for bond lengths and angles for Co–C, Co–N, Co–O, and P–O bonds. These parameters were derived from the X-ray structure of Ado–Cbl [40] (atomic-coordinate file DADCBL in the *Cambridge Crystallographic Data Files*) and from parameters in the Alchemy 3 force field. In addition, the atomic coordinate files CUVCIF and CUVCOL for [(*R*)- and (*S*)-(HO)$_2$pr]–Cbl (**2a**,**b**), resp., [28] were also available.

Enzyme Assays. Assays for glycerol-dehydratase and diol-dehydratase activity with racemic propane-1,2-diol as substrate were performed using a yeast alcohol dehydrogenase/NADH-coupled, UV-based assay system at 37° [26]. A mean rate for the enzyme reaction, measured over the interval $t = 2-3$ min of the assay, was used for the calculation of kinetic constants.

Kinetic Investigations. Apparent inhibition constants (K_i) for **1a**–**d**, **2a**,**b**, and **3a**,**b** were determined by the method applied for the inhibition kinetics of posthomolysis analogues of coenzyme B_{12} (= Ado–Cbl) [26][41]. Ado–Cbl and various amounts of inhibitor were added simultaneously to the assay mixture, and the experiments were repeated at several (usually three) concentrations of Ado–Cbl. Inhibition constants were calculated from linearized data sets in a *Dixon* plot. K_i was computed as the average of the experimental K_i values obtained at different Ado–Cbl concentrations.

We gratefully acknowledge the generous gifts of an *E. coli* strain overexpressing glycerol dehydratase from *Citrobacter freundii* (from Dr. *R. Daniel* and Prof. *G. Gottschalk*, Göttingen, Germany) and a plasmid overexpressing diol dehydratase from *Salmonella typhimurium* (from *T. A. Bobik*, Gainesville, FL, USA). We thank the *European Union* and the *Fonds der Chemischen Industrie* for financial support. *L. P.* thanks the *Alexander von Humboldt Foundation* for short-term postdoctoral fellowships (1996, 1997) and the *Hungarian OTKA* (T023162) and *OMFB* (01789/98) for financial support.

REFERENCES

[1] 'Vitamin B12', Eds. B. Zagalak, W. Friedrich, W. de Gruyter Verlag, Berlin-New York, 1979.
[2] B. M. Babior, J. S. Krouwer, *CRC Crit. Rev. Biochem.* **1979**, *6*, 35.
[3] B. T. Golding, in 'B12', Ed. D. Dolphin, John Wiley & Sons, New York, 1982, Vol. 1, pp. 543–582.
[4] B. M. Babior, *BioFactors* **1988**, *1*, 21.
[5] J. Rétey, in 'Chemical Aspects of Enzyme Biotechnology', Ed. T. O. Baldwin, Plenum Press, New York, 1990, p. 223.
[6] C. D. Garr, J. M. Sirovatka, R. G. Finke, *J. Am. Chem. Soc.* **1996**, *118*, 11142.
[7] C. D. Garr, R. G. Finke, *Inorg. Chem*. **1996**, *35*, 5912.
[8] C. Luschinsky-Drennan, S. Huang, J. T. Drummond, R. G. Matthews, M. L. Ludwig, *Science (Washington, D.C.)* **1994**, *266*, 1669.
[9] F. Mancia, N. H. Keep, A. Nakagawa, P. F. Leadlay, S. McSweeney, B. Rasmussen, P. Bösecke, O. Diat, P. R. Evans, *Structure* **1996**, *4*, 339.
[10] E. Stupperich, H. J. Eisinger, S. P. J. Albracht, *Eur. J. Biochem.* **1990**, *193*, 105.
[11] O. Zelder, B. Beatrix, F. Kroll, W. Buckel, *FEBS Lett*. **1995**, *369*, 252.
[12] R. Padmakumar, S. Taoka, R. Padmakumar, R. Banerjee, *J. Am. Chem. Soc*. **1995**, *117*, 7033.
[13] A. Abend, R. Nitsche, V. Bandarian, E. Stupperich, J. Rétey, *Angew. Chem*. **1998**, *110*, 643; *ibid. Int. Ed*. **1998**, *37*, 625.
[14] M. Yamanishi, S. Yamada, H. Muguruma, Y. Murakami, T. Tobimatsu, A. Ishida, J. Yamauchi, T. Toraya, *Biochemistry* **1998**, *37*, 4799.
[15] C. C. Lawrence, G. J. Gerfen, V. Samano, R. Nitsche, M. J. Robins, J. Rétey, J. Stubbe, *J. Biol. Chem*. **1999**, *274*, 7039.
[16] L. Poppe, E. Stupperich, W. E. Hull, T. Buckel, J. Rétey, *Eur. J. Biochem.* **1997**, *250*, 303.
[17] L. Poppe, H. Bothe, G. Broeker, W. Buckel, E. Stupperich, J. Rétey, *J. Mol. Catal. B*, submitted.
[18] O. Zelder, B. Beatrix, U. Leutbecher, W. Buckel, *Eur. J. Biochem*. **1994**, *226*, 577.
[19] B. Beatrix, O. Zelder, W. Buckel, *Eur. J. Biochem*. **1994**, *221*, 101.

[20] E. N. Marsh, N. McKie, N. K. Davis, P. F. Leadlay, *Biochem. J.* **1989**, *260*, 345.
[21] R. Jansen, F. Kalousek, W. A. Fenton, L. E. Rosenberg, F. D. Ledley, *Genomics* **1989**, *4*, 198.
[22] E. Andrews, R. Jansen, A. M. Crane, S. Cholin, D. McDonnell, F. D. Ledley, *Biochem. Med. Metabol. Biol.* **1993**, *50*, 135.
[23] E. N. G. Marsh, D. E. Holloway, *FEBS Lett.* **1992**, *310*, 167.
[24] T. Tobimatsu, T. Hara, M. Sakaguchi, Y. Kishimoto, Y. Wada, M. Isoda, T. Sakai, T. Toraya, *J. Biol. Chem.* **1995**, *270*, 7142.
[25] M. Seyfried, R. Daniel, G. Gottschalk, *J. Bacteriol.* **1996**, *178*, 5793.
[26] L. Poppe, J. Rétey, *Eur. J. Biochem.* **1997**, *245*, 398.
[27] R. M. Dixon, B. T. Golding, O. W. Howarth, J. L. Murphy, *J. Chem. Soc., Chem. Commun.* **1983**, 243.
[28] N. W. Alcock, R. M. Dixon, B. T. Golding, *J. Chem. Soc., Chem. Commun.* **1985**, 603.
[29] L. Poppe, W. E. Hull, J. Rétey, *Helv. Chim. Acta* **1993**, *76*, 2367.
[30] M. F. Summers, L. G. Marzilli, A. Bax, *J. Am. Chem. Soc.* **1986**, *108*, 4285.
[31] T. G. Pagano, L. G. Marzilli, M. M. Flocco, C. Tsai, H. L. Carrel, J. P. Glusker, *J. Am. Chem. Soc.* **1991**, *113*, 531.
[32] A. Bax, L. G. Marzilli, M. F. Summers, *J. Am. Chem. Soc.* **1987**, *109*, 566.
[33] W. W. Bachovchin, R. G. Eagar, K. W. Moore, J. H. Richards, *Biochemistry* **1977**, *16*, 1082.
[34] H. J. Böhm, G. Klebe, *Angew. Chem.* **1996**, *108*, 2750; *ibid., Int. Ed. Engl.* **1996**, *35*, 2588.
[35] L. Poppe, L. Novák, M. Kajtár-Peredy, C. Szántay, *Tetrahedron: Asymmetry* **1993**, *4*, 2211.
[36] E. Stupperich, H. Eisinger, *Arch. Microbiol.* **1989**, *151*, 372.
[37] E. Stupperich, *FEMS Microbiol. Rev.* **1993**, *12*, 349.
[38] V. Ya Bykhovskii, P. J. Santander, E. Stupperich, N. I. Zaitseva, M. A. Pusheva, E. N. Detkov, D. S. Valyushok, I. A. Scott, *Appl. Biochem. Microbiol.* **1996**, *32*, 179.
[39] R. Daniel, G. Gottschalk, *FEMS Microbiol. Lett.* **1992**, *100*, 218.
[40] P. G. Lenhert, *Proc. Royal Soc. London, Ser. A* **1968**, *303*, 45.
[41] L. Poppe, J. Rétey, *Arch. Biochem. Biophys.* **1995**, *316*, 541.

Received April 21, 1999